Experimental determination of number–phase uncertainty relations

M. Beck, D. T. Smithey, J. Cooper,* and M. G. Raymer

Department of Physics and Chemical Physics Institute, University of Oregon, Eugene, Oregon 97403

Received March 18, 1993

An experimental determination of the uncertainty product for the phase and photon number of a mode of the electromagnetic field is performed. The expectation value of the commutator that sets the lower bound for the uncertainty product is also determined experimentally. This is accomplished by using optical homodyne tomography to measure the density matrix of a small-photon-number coherent state. The experimental results agree with the quantum-mechanical predictions.

If a complete measurement of the uncertainty relation for photon number $\hat{n}$ and the field phase $\hat{\phi}$ is to be performed, it is necessary to develop means for experimentally determining the variances of these quantities, $\Delta n^2 = \langle(\hat{n} - \langle\hat{n}\rangle)^2\rangle$ and $\Delta\phi^2 = \langle(\hat{\phi} - \langle\hat{\phi}\rangle)^2\rangle$, where $\langle\ldots\rangle$ denotes an expectation value. The uncertainty relation is

$$\Delta\phi\Delta n \geq (1/2)|\langle\psi|[\hat{\phi}, \hat{n}]|\psi\rangle|\,, \tag{1}$$

where $|\psi\rangle$ is the state of the field. It can be seen from relation (1) that one also needs to measure the expectation value of the number–phase commutator $[\hat{\phi}, \hat{n}]$, which is an operator and thus is state dependent in general. Previous experiments have measured variances of $\hat{n}$ and $\hat{\phi}$ separately,[1,2] but the commutator expectation value had not been previously measured. We describe an experiment that determines the distributions for the phase and photon number and the commutator expectation for a field containing small numbers of photons. In our approach, the quantities in relation (1) are determined from the experimentally measured quantum state of the field mode. The state is measured with optical homodyne tomography.[3,4] Because the determination of these quantities assumes the validity of quantum mechanics, our method does not provide an independent verification of the uncertainty principle. Our method does provide a measure of how close arbitrary states come to achieving the equality in relation (1). For example, the coherent states are found not to achieve the equality in general. These measurements are in agreement with the quantum-mechanical predictions of the uncertainty principle.

Defining a quantum-mechanical phase of an electromagnetic field has generated much recent interest, and several different phase definitions have been proposed.[1,5,6] In this Letter we use the Pegg–Barnett Hermitian phase operator because of its calculational simplicity.[6] We obtain the phase distribution corresponding to this operator without actually measuring eigenvalues of the operator on individual trials.

The technique of optical homodyne tomography requires that an ensemble of many measurements be performed.[3,4] In this case the relevant interpretation of the uncertainty relation is that the state of the field does not have a well-defined phase and photon number. Quadrature operators for the electric field are defined as $\hat{x} = (\hat{a} + \hat{a}^\dagger)/\sqrt{2}$ and $\hat{p} = (\hat{a} - \hat{a}^\dagger)/i\sqrt{2}$, where $\hat{a}$ is the annihilation operator for a particular spatial–temporal mode of the field. From these operators, rotated quadrature operators can be defined as $\hat{x}_\theta = \hat{x}\cos\theta + \hat{p}\sin\theta$ and $\hat{p}_\theta = -\hat{x}\sin\theta + \hat{p}\cos\theta$. A balanced homodyne detector makes measurements that correspond to the quadrature operator $\hat{x}_\theta$ of the signal field, when the local-oscillator (LO) field is in a large-amplitude coherent state.[7] The spatial–temporal mode of the signal field selected by the homodyne detector is the same as that of the LO,[4] and the measured quadrature is determined by the phase of the LO, θ.

In our experiments an ensemble of measurements of quadrature amplitudes $\hat{x}_\theta$ are made to determine the probability distributions $P_\theta(x_\theta)$ for various values of θ. These distributions can be written in terms of the Wigner function $W(x, p)$ (Ref. 8) of the field mode[3]:

$$P_\theta(x_\theta) = \int_{-\infty}^{\infty} W(x_\theta\cos\theta - p_\theta\sin\theta, x_\theta\sin\theta + p_\theta\cos\theta)\mathrm{d}p_\theta\,. \tag{2}$$

For a set of such probability distributions determined on a continuous set of angles θ, Vogel and Risken[3] showed that one could invert the distributions with the inverse Radon transform to obtain the Wigner function.[3] If distributions are available for a finite and discrete set of angles between 0 and π, the inversion of Eq. (2) can still be performed with numerical techniques familiar in tomographic imaging.[9]

From the measured Wigner function, it is possible to construct the density matrix of the measured field mode by numerically performing a one-dimensional Fourier transform[8]:

$$\langle x + x'|\hat{\rho}|x - x'\rangle = \int_{-\infty}^{\infty} W(x, p)\exp(2ipx')\mathrm{d}p\,. \tag{3}$$

Because the density matrix completely determines the quantum-mechanical state of a system, optical homodyne tomography provides a way to determine this state. The density matrix of Eq. (3) can be expressed in the representation of the number states $|n\rangle$

0146-9592/93/151259-03$6.00/0

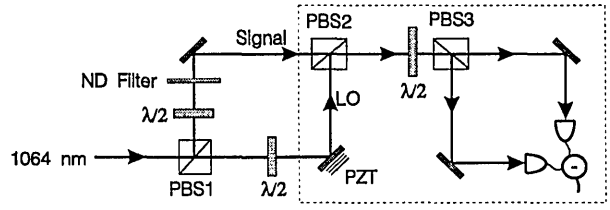

Fig. 1. Experimental apparatus. The dashed lines enclose the balanced homodyne detector.

through a change of basis by computation of overlap integrals of the density matrix in the x representation with Hermite polynomials.

In our experiment, the signal field was prepared in coherent states of differing average photon number. The experimental layout for measuring the field state is shown in Fig. 1. A Nd:YAG laser produces 300-ps, nearly transform-limited pulses at 1064 nm with a repetition rate of 420 Hz and a pulse-energy stability of ±3%. The pulses are split with a polarizing beam splitter (PBS1) to create the signal and the LO beams. Half-wave plates and neutral-density (ND) filters in each arm are used to control the relative intensities of these two beams. The piezoelectric translator (PZT) pushes a mirror that adjusts the phase of the LO. Each LO pulse contains approximately 2×10^6 photons, whereas the number of photons in the signal pulse is varied between 0 and ~10. The signal and LO beams are superimposed with orthogonal polarizations on a polarizing beam splitter (PBS2). Our balanced homodyne detector consists of a half-wave plate that rotates the polarizations of the signal and the LO fields by 45° and a polarizing beam splitter (PBS3) that interferes the signal and the LO to produce two output fields that are detected by high-quantum-efficiency (~85%) InGaAs photodiodes. The photodiode outputs are electronically subtracted and integrated with a low-noise charge-sensitive preamplifier.[10] For each laser pulse this subtracted and integrated signal yields the photoelectron difference number between the outputs of the two detectors. This balancing arrangement removes most of the additive classic noise on the LO and allows us to make measurements at the shot-noise level[11] (SNL). The electronic noise variance is approximately six times lower than the LO SNL, which is defined as the variance of photoelectron counts from a coherent-state LO.

For each coherent state with mean photon number $\bar{n}$, we make 5000 repeated measurements of the photoelectron difference number N_θ at 11 values of the LO phase equally spaced in a $[0, \pi]$ interval and calculate photoelectron distributions $P_{N_\theta}(N_\theta)$. The variance of each of these photoelectron distributions yields the SNL of the LO, denoted by $\bar{n}_{\mathrm{LO},\theta}$. The difference number is scaled to yield the quadrature amplitude with $x_\theta = N_\theta/(2\bar{n}_{\mathrm{LO}})^{1/2}$, where $\bar{n}_{\mathrm{LO}}$ is the average of the 11 values of $\bar{n}_{\mathrm{LO},\theta}$. We can determine the LO SNL, $\bar{n}_{\mathrm{LO}}$, in an independent manner by blocking the signal beam and one detector and directly measuring the number of LO photoelectrons that hit the other detector. Because the detectors are balanced, the total number of LO photoelectrons is twice this measured number. These two methods of obtaining the scaling factor $(\bar{n}_{\mathrm{LO}})^{1/2}$ agree to within 4%.[10] Scaling $P_{N_\theta}(N_\theta)$ then yields the distributions $P_\theta(x_\theta)$ of the quadrature amplitudes. From these distributions we use the inverse Radon transform to calculate the Wigner function, as described above. When performing the numerical inversion to obtain the Wigner function, we use the standard filtered backprojection algorithm for parallel-beam sampling geometry.[9]

We then extract the density matrix by using Eq. (3). A sufficient condition that a density matrix describes a pure state is $\mathrm{Tr}(\hat{\rho}^2) = 1$. When these traces are calculated for our experimentally determined density matrices, they are found to equal 1.00 ± 0.02, and consequently we conclude that our state is pure. From the measured density matrix we can calculate $\Delta\phi$, Δn, and $|\langle[\hat{\phi}, \hat{n}]\rangle|$.

When calculating moments of the signal photon number, we find it best not to use the photon-number distributions obtained from the density matrix. The reason for this is that the distributions do not decay completely to zero, and they must thus be truncated at some point; hence the moments of $\hat{n}$ are sensitive to exactly where the distribution is truncated. To avoid this problem, we write the photon-number operator $\hat{n} = \hat{a}^\dagger\hat{a}$ in terms of the quadrature operators, $\hat{n} = (1/2)(\hat{x}^2 + \hat{p}^2 - 1)$. The quadrature operators are then placed in Weyl order, and the moments are calculated as c-number integrals of the measured Wigner function.[8] Using these moments, we calculate the mean and the variance of the photon number. We estimate the mean to be accurate to better than 8%, limited by drift and noise of the LO pulses and the electronics as well as by the finite number of $P_\theta(x_\theta)$ distributions. An independent, but less accurate, check of the mean photon number yields results a factor of ~1.7 greater than that measured with the Wigner function.

The Pegg–Barnett Hermitian phase operator $\hat{\phi}$ is defined in a finite (but arbitrarily large) dimensional Hilbert space.[6] In an $(s + 1)$-dimensional Hilbert space, the phase states are defined as

$$|\phi\rangle = \frac{1}{\sqrt{s+1}} \sum_{n=0}^{s} \exp(in\phi)|n\rangle. \tag{4}$$

This Hilbert space is spanned by a complete orthonormal set of basis-phase states $|\phi_m\rangle$, given by Eq. (4) with ϕ replaced by $\phi_m = \phi_0 + 2\pi m/(s + 1)$, with $m = 0, 1, \ldots, s$ and ϕ_0 a reference phase. In terms of the states $|\phi_m\rangle$, the Hermitian phase operator is then

$$\hat{\phi} = \sum_{m=0}^{s} \phi_m|\phi_m\rangle\langle\phi_m|. \tag{5}$$

With this definition, the phase states are the eigenstates of the phase operator, i.e., $\hat{\phi}|\phi\rangle = \phi|\phi\rangle$. In our experiments, ϕ actually corresponds to the phase difference between the signal and the LO field. The normalized phase distribution for a state described by $\hat{\rho}$ in the number-state representation is

$$\begin{aligned} P_{pb}(\phi) &= [(s + 1)/2\pi]\langle\phi|\hat{\rho}|\phi\rangle \\ &= \frac{1}{2\pi} \sum_{n,m=0}^{s} \exp[i(m - n)\phi]\langle n|\hat{\rho}|m\rangle. \end{aligned} \tag{6}$$

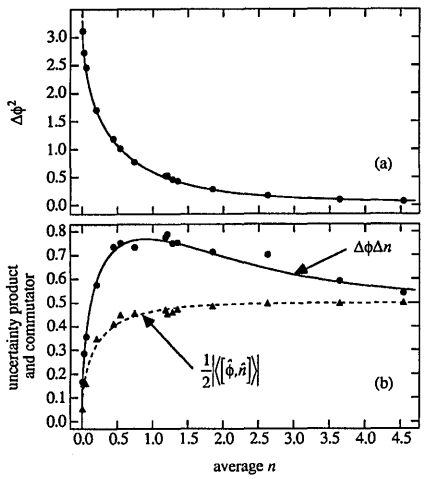

Fig. 2. (a) Variance of the phase plotted against the average number of photons in a coherent state. The points are the experimentally determined values, and the solid curve is calculated from the theory for the Pegg–Barnett phase definition. (b) Points are experimentally determined values for the uncertainty product (circles) and the commutator expectation (triangles). The curves are the theoretical values for the uncertainty product (solid curve) and the commutator expectation (dashed curve).

For all the coherent states we have measured ($\bar{n} \leq 8$), this distribution converges for $s \geq 20$.

Once the phase distributions are computed, moments of the phase can be calculated. The measured variances of the Pegg–Barnett phase as a function of the mean number of photons in the signal field are shown in Fig. 2(a). The theoretical variances for a coherent-state signal field are also plotted in Fig. 2(a).[12] Agreement between the experimental data and the theory is good and indicates that the states that we are measuring in the experiment are well described by pure coherent states.

Both the uncertainty product $\Delta\phi\Delta n$ and the expectation value of the commutator $(1/2)|\langle[\hat{\phi}, \hat{n}]\rangle|$ for our experimentally measured data are plotted in Fig. 2(b). For the experimental data we calculate the commutator expectation value numerically by expressing the matrices for $\hat{\phi}$ and $\hat{n}$ in the number-state representation, evaluate the matrix that corresponds to the commutator, and trace the commutator over the measured-density matrix in the number-state representation. Also plotted are the theoretically predicted values for coherent states. For the theoretical uncertainty product, $\Delta\phi$ is calculated in the same fashion as used to generate Fig. 2(a), whereas the photon-number standard deviation is $\Delta n = \sqrt{\bar{n}}$ for a coherent state. The equation describing the theoretical commutator is found in Ref. 6. Note that the uncertainty relation is satisfied (as it must be with our method of analysis); the uncertainty product is greater than the expectation value of the commutator. This means that, despite their purity, coherent states are not intelligent states with respect to number and phase. Intelligent states are defined as states for which relation (1) is an equality.[13] The only coherent state that is a minimum-uncertainty state is the vacuum, for which $\Delta\phi\Delta n = 0$. It is seen, however, that, in the limit of very small or very large coherent-state amplitude, the coherent states are approximately number–phase intelligent.

In conclusion, we have developed a technique for experimentally determining the standard deviation of the phase $\Delta\phi$ and the photon number Δn, as well as the expectation value of their commutator $|\langle[\hat{\phi}, \hat{n}]\rangle|$, for a mode of an optical field. We have thereby measured, for the first time to our knowledge, the number–phase uncertainty relation, which is in general state dependent. This method of field characterization will work in principle for arbitrary states of the field—the only limitation being available experimental parameters (e.g., detector efficiency, resolution). Agreement between the measured and theoretical points in Fig. 2 is ensured by agreement between the measured and theoretical density matrices. Therefore other phase definitions could be used, also leading to good agreement of experiment and theory. For this reason, our results do not favor one phase definition over another.

We acknowledge several helpful discussions with A. Faridani, H. Carmichael, and W. Schleich. This research is supported by National Science Foundation grant PHY 8921709-01.

*Permanent address, Joint Institute for Laboratory Astrophysics and the Department of Physics, University of Colorado and the National Institute of Standards and Technology, Boulder, Colorado 80309.

References

1. J. W. Noh, A. Fougeres, and L. Mandel, Phys. Rev. Lett. **67,** 1426 (1991); Phys. Rev. A **46,** 2840 (1992).
2. H. Gerhardt, U. Buchler, and G. Litfin, Phys. Lett. A **49,** 119 (1974); M. M. Nieto, Phys. Lett. A **60,** 401 (1977).
3. K. Vogel and H. Risken, Phys. Rev. A **40,** 2847 (1989).
4. D. T. Smithey, M. Beck, A. Faridani, and M. G. Raymer, Phys. Rev. Lett. **70,** 1244 (1993).
5. L. Susskind and J. Glogower, Physics **1,** 49 (1964); J. H. Shapiro and S. R. Shepard, Phys. Rev. A **43,** 3795 (1991).
6. D. T. Pegg and S. M. Barnett, Phys. Rev. A **39,** 1665 (1989); J. Mod. Opt. **36,** 7 (1989).
7. H. P. Yuen and J. H. Shapiro, IEEE Trans. Inform. Theory **IT-26,** 78 (1980).
8. M. Hillery, R. F. O'Connell, M. O. Scully, and E. P. Wigner, Phys. Rep. **106,** 121 (1984).
9. F. Natterer, *The Mathematics of Computerized Tomography* (Wiley, New York, 1986); A. Faridani, in *Inverse Problems and Imaging; Pitman Research Notes in Mathematics,* G. F. Roach, ed. (Wiley, Essex, England, 1991), Vol. 245, p. 68.
10. D. T. Smithey, M. Beck, M. Belsley, and M. G. Raymer, Phys. Rev. Lett. **69,** 2650 (1992).
11. H. P. Yuen and V. W. S. Chan, Opt. Lett. **8,** 177 (1983).
12. R. Lynch, Phys. Rev. A **41,** 2841 (1990).
13. J. A. Vaccaro and D. T. Pegg, J. Mod. Opt. **37,** 17 (1990).